FEATURE ARTICLE

Check for updates

Electronic effects and fundamental physics studied in molecular interfaces

Thomas Pope, [ID] [a] Shixuan Du, [ID] [b] Hong-Jun Gao [ID] *[b] and Werner A. Hofer [ID] *[ab]

Scanning probe instruments in conjunction with a very low temperature environment have revolutionized the ability of building, functionalizing, and analysing two dimensional interfaces in the last twenty years. In addition, the availability of fast, reliable, and increasingly sophisticated methods to simulate the structure and dynamics of these interfaces allow us to capture even very small effects at the atomic and molecular level. In this review we shall focus largely on metal surfaces and organic molecular compounds and show that building systems from the bottom up and controlling the physical properties of such systems is no longer within the realm of the desirable, but has become day to day reality in our best laboratories.

Introduction

It is quite striking to consider the evolution of surface physics and chemistry over the last two decades. At the end of the 1990s it was barely possible to structure single atom arrays on surfaces *via* hugely time-consuming manipulations of atoms with the help of the tip of a scanning tunnelling microscope (STM),[1,2] or perform simple chemical reactions *in situ*.[3] Chemistry, one could say was largely present as physical chemistry and the height of sophistication was to manipulate small molecules consisting of a few atoms. A carbon monoxide molecule, in this context, was considered a complicated entity, sometimes called the fruit fly of surface science, as the fruit fly was similarly ubiquitous in genetic research.

This has changed dramatically in the early 2000s, as scientists began to imitate the much more sophisticated and varied mechanisms by which molecules interact in biological systems, where, for example, hydrogen bonding is essential for the functioning of living organisms in the form of DNA.[4] With more refined methods of molecular organisation came an approach to two dimensional interfaces, which was no longer dependent on the engineering of a particular atomic or molecular order by physical means like heat or atomic and molecular forces, but an approach which largely determined the ensuing organisation of an interface by the selection of particular components, whether these were specific surfaces, a specific atomic arrangement on a surface, the atoms and molecules constituting the interface, and the specific forms in which these atoms and molecules interact

with each other and a particular surface. Given the possibilities in surface physics and chemistry and the prowess of organic chemists in synthesizing new components, the variety of self-assembled interfaces today is near infinite.

At the same time, a similar change in methods and abilities occurred in theory. At the end of the 1980s quantum chemistry methods like Hartree–Fock[5,6] or atomic orbital based simulations were still widely used by the surface physics and physical chemistry community, because methods which were in principle more precise, like density functional theory[7,8] (DFT), were still too expensive to run for large systems. Even at the beginning of the 1990s DFT was limited to the simulation of about 100–200 atoms in a highly regular crystal lattice.[9] The decisive technology changes, which rapidly transformed the field in this area, and led to the widespread adoption of the DFT method,[10,11] were pseudopotentials and a parallel computing environment.

Proposed in the 1930s,[12,13] and becoming widely used in the 1990s,[14] pseudopotentials removed the need to simulate the core regions of atoms, which had made computations faced with two separate physical environments and complicated boundary conditions at the interface very costly. Based on a continuation of potentials in the valence range into the atomic cores by much simpler functions than *e.g.* Coulomb potentials, pseudopotential simulations generate a single and much simpler physical environment.[15,16] On this basis methods in DFT could use plane waves, which are ideal for systems with periodic boundaries and easy to integrate.[17,18] Moreover, a formulation for creating pseudopotentials *via* quasi wavefunctions in the core environment, the projector augmented wave method, was suitable to also simulate magnetic systems, which pseudopotentials previously were incapable of.[19,20]

High performance computing, which only became widely available in the new millennium, allowed to structure theoretical

[a] School of Natural and Environmental Sciences, Newcastle University, Newcastle upon Tyne NE1 7RU, UK. E-mail: werner.hofer@newcastle.ac.uk

[b] Institute of Physics & University of Chinese Academy of Sciences, Chinese Academy of Sciences, P.O. Box 603, Beijing 100190, China. E-mail: hjgao@iphy.ac.cn

methods in highly parallel and efficient coding, which again profited from the usage of plane waves. Routines today are parallelized either *via* the Brillouin zone integration[17] and the *k*-point sampling, or they are parallelized over the plane wave components of the DFT orbitals.[17] It is not uncommon today to have simulation runs performed in parallel on hundreds of computing cores. In conjunction with very fast processor tact rates and interconnects being able to shift gigabits of data from one computing core to the other in less than a second, we are today able to simulate thousands of atoms reliably and in a reasonable time. This means, that for the first time in about hundred years, experiments and simulations in this field can be undertaken simultaneously. This, we think, is decisive for the successful interaction between them. Furthermore, while the long-promised general orbital-free linear scaling method remains elusive,[21–23] with the rise in order-N techniques,[24,25] linear scaling simulations can be performed on systems with non-zero band-gaps, conditionally allowing calculations to be run on tens of thousands of atoms.

In this review we want to trace some of the progress made in the last decade by combining different substrates with a wide variety of engineered molecules to create novel interfaces. All experiments were performed using scanning tunnelling microscopy (STM) and scanning tunnelling spectroscopy (STS), typically in combination with high-level density functional theory simulations and mostly in a low-temperature environment. The availability of He^3 dilution fridges, which allow to take the operating temperature in the measurements to below 0.4 K proved a crucial improvement in particular for the understanding of subtle electronic and vibrational effects. We have, where possible, included the relevant work of colleagues with a view of providing a snapshot of the field not just from the perspective of our own work, but of the work of the whole community in surface physics and chemistry engaged in the ambitious project of crossing the next frontier in the engineering of atoms and molecules from the bottom up.

We shall address interactions of the various components of a surface/interface system in the following sections and show how each of them leads to particular composition of the interface and particular physical effects that can be studied using scanning probe instruments.

Substrate topology

Gold has been used as a substrate for atomically resolved experiments in surface physics for at least 30 years, since the first atomically resolved image of a close packed Au(111) surface could be obtained.[27] Perfect gold surfaces are largely inert,[28] but their reactivity changes upon reconstruction,[29] and gold surfaces are catalytically highly active for gold nanoparticles.[30] Typically gold surfaces reconstruct in a herringbone structure, where the most reactive points, usually the points of molecular attachment, are the elbows of the herringbone.[31]

C60 fullerenes, discovered in the 1980s,[32] have been used to create molecular interfaces on gold since the 1990s, when it was noted that they favoured being selectively anchored at the lower step edges.[33,34] This experimental result suggested that vicinal Au surfaces were an ideal substrate for ordered assembly of fullerenes. Employing Au(12 11 11), C60 molecules can be deposited to form short chains of mostly four and five units in length.[35] It was noted that the C60 molecule is exclusively adsorbed on the fcc areas of the step, owing to the possibility of charge transfer between the electron-rich step edge and the electron-deficient C60 molecule. There is a rich literature on C60 molecular interfaces, not only on gold but also on other surfaces like copper,[36] and the molecules continue to attract considerable attention due to their ability to be functionalized *e.g.* by trapping atoms internally to form endohedral fullerenes.[37]

The use of monoatomic step-edges and vicinal surfaces has been widely researched[38,39] as a template for self-assembly of atomic chains[40–42] and of supramolecular chains.[43] It was shown that these step edges were ideal for highly site-specific and single-orientation adsorption of hexa-*peri*-hexabenzocoronene (HBC),[44] a molecule that is able to accommodate different functional groups[45–49] and thus modify the functional and mechanical properties of the molecule. These two properties make HBC-molecules a potential anchor in multicomponent supramolecular networks when extended with appropriate functional side groups.

If a molecule physisorbs to the step-edge of a substrate surface, it sometimes alters the atomic position of the step-edge atoms in a particular way. This has been shown, for example, on Cu(110) surfaces, using metal-phthalocyanine.[50] Exploiting the particular molecular geometry of chiral geodesic hydrocarbon hemibuckminsterfullerenes, the structure of a Cu(110) surface is remodelled in such a way that the chirality is imprinted onto the substrate.[26] Fig. 1 shows this restructuring, where the step edges (a) are favoured by either minus (*M*) or plus (*P*) enantiomers (b). The surface structure is remodelled into islands consisting of step-edges with a chirality dictated by the molecules (c and d). These structures are observed experimentally by STM imaging (e–g). Given the role of chirality-induced spin selectivity,[51–53] the ability to impart chirality onto metal surfaces opens up a promising avenue for tailoring the magnetic structure of interfaces at the atomic scale for particular applications.

In addition to its position and orientation, the ability to control the motion of a molecule plays an important role in molecular engineering.[56,57] In particular, a high level of control over the axis of rotation is important for molecular rotors,[58] which are vital precursors to molecular machines. While previous work had identified molecular rotors, they had largely studied systems with no fixed axis.[59–62] In 2008, it was shown that tetra-*tert*-butyl zinc phthalocyanine molecules on an Au(111) surface exhibited a well defined contact point with a gold adatom, leading to a fixed off-centre rotation axis,[54] seen in Fig. 2(e and f). It was also noted that single-molecule rotors form large scale ordered arrays due to the reconstruction of the gold surface (see Fig. 2(a)). Similar arrays have since been reported[63] as well as supramolecular rotors caged in network pores.[64–66]
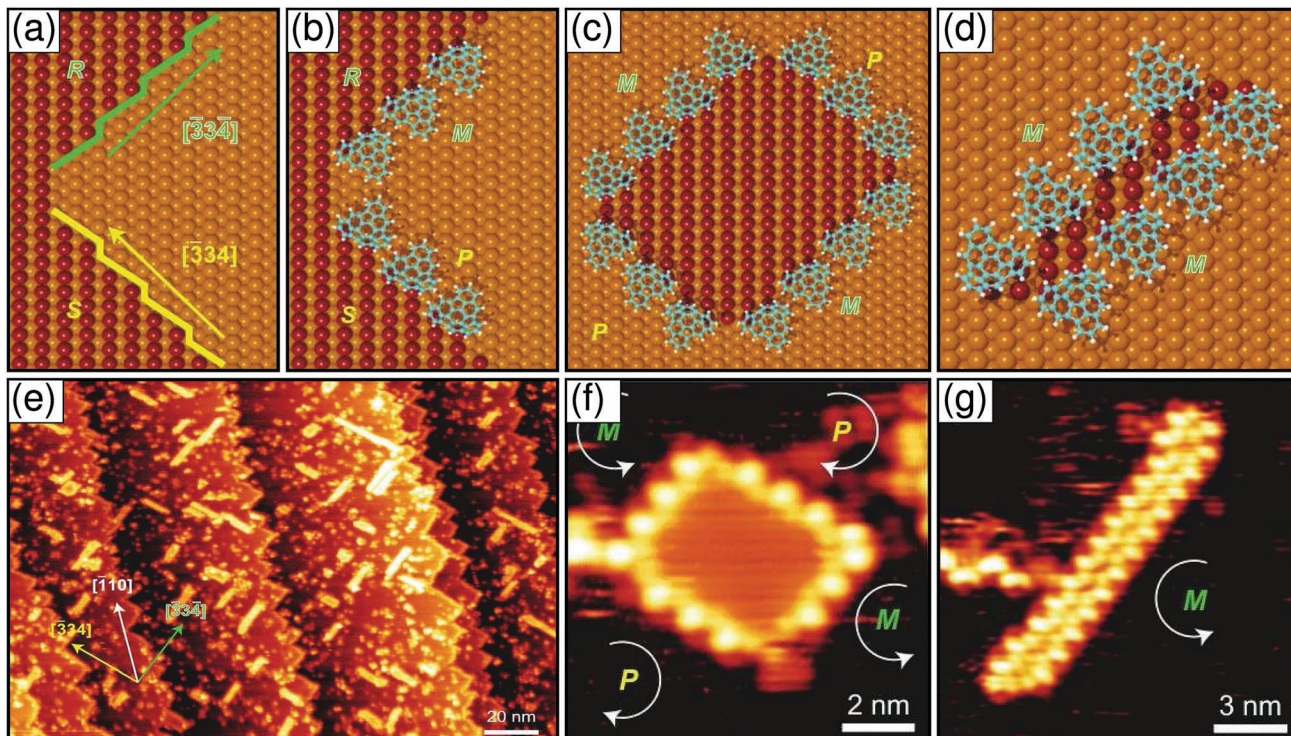
Fig. 1 Structure models for homochiral step edges. (a) Hard-sphere model of the observed step edge with alternating [$\bar{3}\bar{3}4$] and [$\bar{3}34$] segments and the formation of chiral kink sites. (b) Structure model of the observed hemifullerene-decorated steps along [$\bar{3}\bar{3}4$] and [$\bar{3}34$]. Minus (M) enantiomers decorate R kinks ($\bar{3}\bar{3}4$), and plus (P) enantiomers decorate S kinks ($\bar{3}34$). (c) Structural model of an adatom island stabilized by M- and P-hemifullerene. (d) Structural model of an M-hemifullerene-stabilized Cu adatom nanowire running along the [$\bar{3}\bar{3}4$] direction. (e) STM image (U = −2.0 V, I = 22 pA, T = 50 K) acquired after the deposition of 15% of a complete monolayer of hemifullerene at room temperature. Instead of linear step edges along [$\bar{1}11$], as observed for clean Cu(110), the step edges are decorated with molecules and have a zigzag shape that exhibits [$\bar{3}\bar{3}4$] and [$\bar{3}34$] directions. On the (110) terraces, single molecules, nanowires and elongated islands with edges aligned along the [$\bar{3}\bar{3}4$] and [$\bar{3}34$] directions are observed. (f and g) Enantioselective step decoration of 2D Cu islands and Cu metal wires. Steps and wires running parallel to the [$\bar{3}\bar{3}4$] direction are decorated with M enantiomers, and those running parallel to the [$\bar{3}34$] direction are decorated with P enantiomers (T = 300 K, U = −2.0 V, I = 23 pA for (f), and U = −2.4 V, I = 35 pA for g and h). Adapted from Xiao et al.[26] with permission from Springer Nature, copyright 2016.

Caging molecules within a network of pores is a widely exploited technique, with work focusing on the caging of C60 molecules,[67–69] CO[70] molecules and others.[71] Beyond the obvious advantage of constructing a predefined lattice for the functional molecules to occupy, there are some interesting additional considerations. The impact of molecule–molecule interaction must be understood and is explored in more detail in a later section. The effect of the network structure on the substrate must also be considered. For example, recent work confining magnetic atoms inside quantum corals has shown that the nature of the Kondo feature is tunable by manipulation of the underlying surface states.[72] Since the chemistry and topology of the surface is affected by the network lattice, the chemistry of the monolayer will play a crucial role beyond its immediate topological impact.

Similar to the idea of constructing a network of pores from a molecular monolayer, the well known moiré structure of graphene supported on ruthenium(0001)[73–77] (G1/Ru(0001)) provides an interesting topology onto which metal atoms can be deposited. This approach has been identified as a valuable template for metal clusters.[76,78–84] In an extensive DFT analysis, Zhang et al. showed that Pt, Ru, Ir and Ti atoms selectively adsorb on the fcc region and Pd, Au, Ag and Cu atoms form non-selective structures owing to their fully occupied d-orbitals.[55] The growth path of Pt nanoclusters is shown in Fig. 3 as an example. In general, the local sp^3 hybridization of the graphene substrate and the occupation of the outermost metal orbital were found the be determining factors in the formation of the nanoclusters, allowing for a predictive model for selecting appropriate graphene–metal combinations as a substrate in order to form ordered arrays of nanoclusters.

The topology of graphene/Ru(0001) can even be used to adsorb and order molecules. Similar patterns have been seen in BN/Ru(0001),[85] BN/C(111),[86] BN/Ir(111)[87] and BN/Rh(111),[88] with the latter two shown to be a good template for the formation of cobalt phthalocyanine and C60 monolayers respectively. For graphene/Ru(0001), it has been shown, for instance, that iron phthalocyanine molecules adsorbed on the graphene monolayer will generate large scale Kagome lattices.[89] Kagome lattices, or lattices composed of triangles and hexagons, are extremely rare in the two dimensional organisation of molecules and typically achieved by metal–organic coordination. On a graphene monolayer they are due to the highly variable electric dipole moments induced by charge redistribution in the interface of graphene and ruthenium.[90]
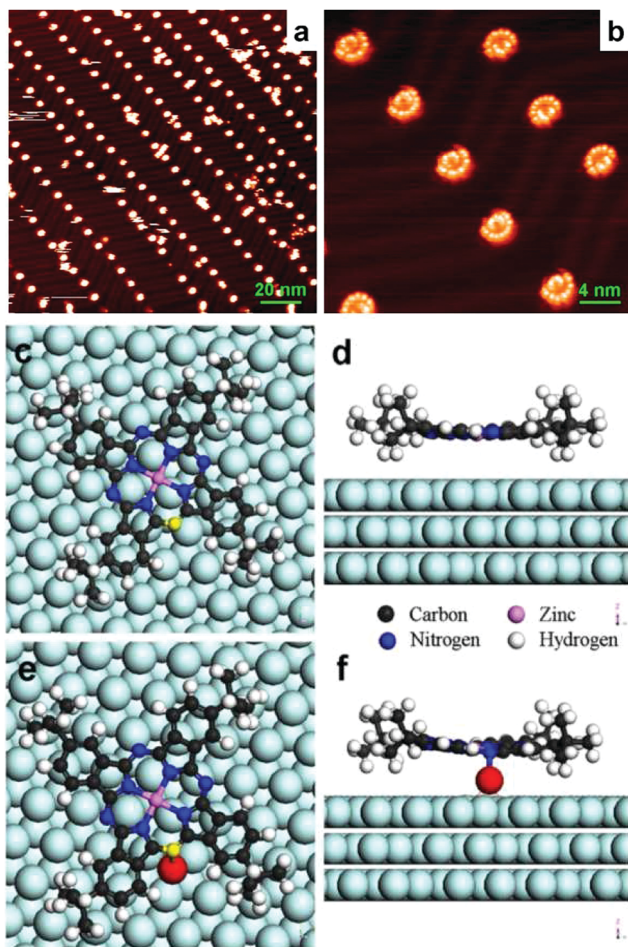
Fig. 2 (a) STM image of large scale ordered array of single $(t\text{-Bu})_4$–ZnPc molecular rotors on the reconstructed Au(111) surface. (b) High-resolution STM image of single molecular rotors showing a "folding-fan" feature. The molecular rotors at two different elbow sites show different features due to the modulation by corrugation ridges. Scanning parameters: $U = -1.3$ V, $I = 0.07$ nA. Images were taken at 78 K. (c) Top view and d, side view of the optimized adsorption configuration of a $(t\text{-Bu})_4$–ZnPc molecule on the released Au(111) surface. (e) Top view and (f), side view of the optimized configuration of a $(t\text{-Bu})_4$–ZnPc molecule adsorbed on the Au(111) surface *via* a gold adatom. The molecular formula of $(t\text{-Bu})_4$–ZnPc is $C_{48}H_{48}N_8Zn$. Adapted from Gao et al.[54] with permission from American Physical Society, copyright 2008.

Fig. 3 Schematics of the layer by layer growth path of Pt nanoclusters on the fcc region of the G/Ru(0001) from one Pt atom (a) to sixteen Pt atoms (g) and (d) shows the metastable configurations for four and sixteen Pt atoms on G/Ru(0001). (h) The stable configuration of sixteen Pt atoms on G/Ru(0001). (i) Average binding energy (E_{ab}) vs. the number of the Pt atoms, the black and red squares show the E_{ab} of Pt atoms located at the first and second layer, respectively, where the dashed line at 5.84 eV shows the cohesive energy of Pt. Adapted from Zhang et al.[55] with permission from John Wiley and Sons, copyright 2014.

Substrate chemistry

While the topology of the substrate can clearly have an impact on the structure of the adsorbate, a more subtle effect can be seen in the interplay between the molecules and the substrate chemistry. Famously, adatoms can be used to confine the surface state electrons into quantum corrals[1] and it has been shown that these surface states can affect the positioning on single adatoms.[92–94] This effect has also been observed in molecules like carbon monoxide[95] and, in 2009, it was shown that cobalt-phthalocyanine (CoPc) on Cu(111) arranges due to electron interference mediated by the substrate.[96] At low coverage, Friedel-type oscillations[97] were observed around each CoPc molecule. As the coverage was increased, the molecules formed a pattern with hexagonal symmetry similar to that of Cu atom
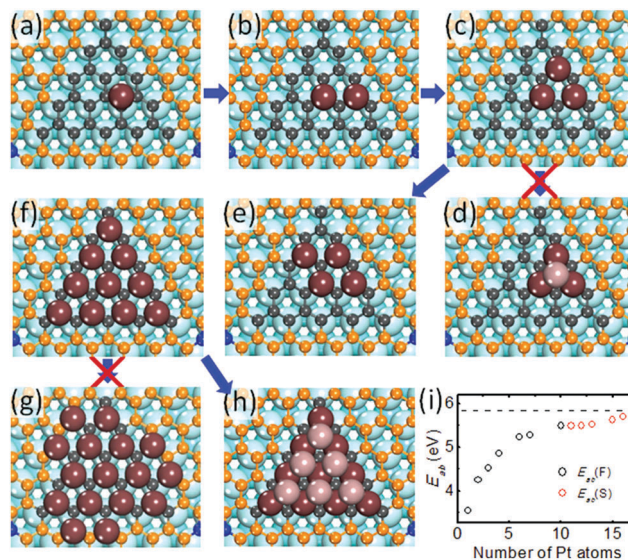
assemblies on Cu(111)[92] and Br island arrays on Cu(111).[98] As the coverage is further increased, the molecules form an array of chains and, at 0.8ML, the molecular superstructure formed a kagome network, stabilized by surface-state mediated interactions. This conclusion was supported by a molecule–molecule nearest neighbour separation histogram, which exhibited the tell-tale oscillatory trend of electron scattering substrate-mediated interactions.

In addition to the underlying electron surface states, the substrate temperature is expected to be an important factor since it determines the rate of surface diffusion, nucleation, dissociation, deposition and the speed of structural relaxation. A study of Coronene on Ag(110) exhibited this temperature dependence.[91] Fig. 4 shows the two monolayer structures found for Coronene on Ag(110) as well as their calculated free energies, which shows that, at 377 K, the most stable configuration swaps from one structure to the other. The molecule forms two structures (I and II) on the substrate. A molecular monolayer is grown at 250 K in I, but increasing the temperature to 335 K causes a transition to II due to the different vibrational contributions to the free energy of structures I and II. Finally, at 367 K, molecule–molecule repulsion causes a transition back to structure I. This temperature dependence has been noted in other molecules.[99,100]

The electronic structure and fundamental physical properties of 2-d systems

Molecule–molecule interactions

For molecules that bind only weakly to the substrate, the dominant mechanism in forming monolayers is the molecule–molecule
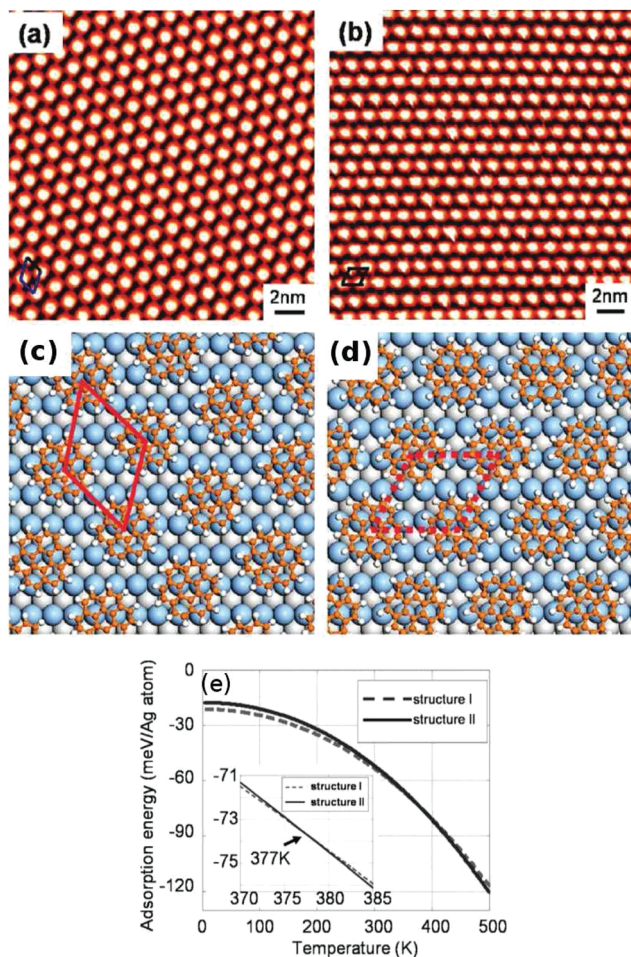
Fig. 4 (a and b) STM images of structures I and II, respectively (scanning parameters: area = 22 × 22 nm, $V = -1.12$ V, $I = 0.08$ nA), the unit cells of structures I and II are marked separately in the bottom-left of the images. Parts c and d, the calculated fully relaxed configurations of structures I and II, respectively, the unit cells are marked. (e) Calculated free energies of structures I and II *versus* temperature. For a dense molecular overlayer, structure I is favoured from 0 to 377 K, structure II is favoured above 377 K. The inset shows the zoomed-in curves between 370 and 385 K. Adapted from Shi *et al.*[91] with permission from American Chemical Society, copyright 2009.
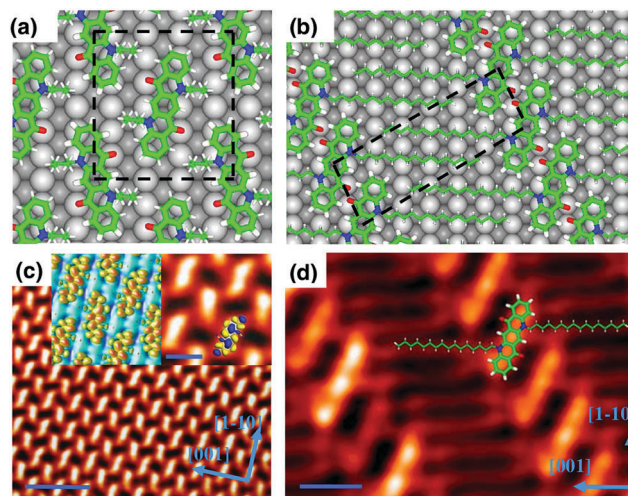
Fig. 5 Comparison of simulated and experimental STM images. (a and b) Predicted geometry of QA4C and QA16C monolayers on Ag(110). (c) Large scale STM image of QA4C. High resolution experimental scans [right inset in (c)] in good agreement with simulations [left inset in (c)]. Tunnelling current in (c): 0.25 nA, bias voltage on sample: 1.3 V and scale bar: 1 nm for (c) left inset and 5 nm for (c). The inset in the right inset of (c) is the LUMO of the QA4C molecule. (d) STM image of QA16C at 77 K which precisely fits the predictions in (b). The tunnelling current is 0.04 nA and 0.8 V for sample bias. The scale bar is 1 nm. Adapted from Shi *et al.*[101] with permission from American Physical Society, copyright 2006.

interaction. It was shown, for example, that thanks to weak binding to the Ag(111) substrate, the arrangement of tetra-pyridyl-porphyrin (TPyP) and Fe(II)-tetra-pyridyl-porphyrin (Fe-TPyP) molecules is mainly determined by intermolecular interactions,[102] though the orientation of the TPyP molecule is largely determined by the its coupling to the substrate.[103]

Decorating molecules with side-groups is an effective method for tuning their arrangement in monolayers. One such method is to attach alkyl chains of various lengths. The arrangement of quinacridone derivatives (QA) with alkyl chains of 4–16 carbon atoms on Ag(110) substrate was shown to depend on the length of the alkyl chains[101] (see Fig. 5). While the oxygen on the molecule determines how it binds to the surface, the chains determine the arrangement of the molecules with respect to each other. It was also shown that the elastic properties – like the

Youngs modulus – are tunable by varying the length of the alkyl side chains.[104] Research into the mechanical tunability of mono-layers in this way is still very limited.[105–107]

In studying the arrangement of molecules into more than one layer, the effect of the substrate inevitably diminishes as more layers are considered. This was noted in the case of tin-phthalocyanine (SnPC) adsorbed onto Ag(111).[108] Due to its non-planer structure, SnPC can adsorb with the Sn atom either above or below the molecular plane (Sn-up and Sn-down respectively). The incommensurate monolayer phase exclusively consists of the Sn-down configuration, while a mixture is found in the commensurate low-temperature submonolayer phase.[109–111] It was shown that at low coverage, the SnPC-up molecules were isolated, whereas the SnPC-down configuration formed chains[108] and alternating chains of SnPC-up and -down where observed in the monolayer phase.[112] Finally, while the mixed configuration exists for the first two layers, at higher coverage, the layers consist of single-configuration structures, where the third and forth layers favours the SnPC-up and SnPC-down configurations respectively.[108] Similar behaviour was reported on Au(111).[113]

Extending the idea of multi-layer configurations, one might consider the effect one monolayer would have on a second consisting of different molecules. Work has shown that in addition to network pores, functional molecules may occupy specific sites atop an underlying monolayer.[116–118] In addition, a significant amount of research has focused on the stacking of covalently bonded nanolayers like Boron Nitride and Graphene[119,120] and other nanosheets.[121] The unique inter-action between these monolayers opens up an promising new field of research.

Electronic effects I: Kondo resonances

One of the first observations of a Kondo resonance was the measurement of a dI/dV spectrum of a single Co atom on a Au(111) surface.[122] Instead of a simple Lorentzian peak, a Fano resonance[123] was observed, which typically arises due to the interference between two available tunnelling channels. It was proposed that the first channel was due to the surrounding continuum of conduction band electrons, while the second was associated with the d-orbitals in the Co atom. Similar observations at this time were reported for Ce atoms on a Ag(111) surface[124] and later experiments found Kondo resonances associated with Ni, Co and Ti atoms on a Au(111) surface.[125] However, this latter study was unable to observe Kondo resonances for Fe, Mn, Cr or V atoms due to their low Kondo temperature, and the experimental limitation at that time to temperatures above typically 5 K. Later studies showed that the Kondo temperature could be modified by caging the atoms in molecules.[126] To this end, iron phthalocyanine molecules were studied and it was found that the dI/dV spectra in this case exhibited the typical Fano resonance.[114] The molecule was shown to have two site-specific behaviours associated with two configurations, I and II. The first has an implied Kondo temperature of 357 K and the second of 598 K, which was attributed to a difference in the spin-electron coupling. However, as experimental techniques evolved and dilution fridges operating at 0.4 K became more widely available,[127] it was discovered that this feature in the spectrum was not in fact a Kondo resonance.[128] The perceived Kondo resonance at 5 K was shown to be the envelope in the spectra of a much sharper feature, which only became apparent at very low temperature. Fig. 6 shows this for two absorption configuration for FePc molecules on Au(111). From the viewpoint of basic physics this new interpretation was also better aligned with the general properties of Kondo resonances, which depend on the coupling between the spin state of an atom or molecule and the conduction band of a metal: for very low coupling, as in case of molecular physisorption on a flat metal surface, one would expect a fairly low coupling and consequently a low Kondo temperature. Today, it is understood that Kondo temperatures in such systems rarely have a value exceeding 10 K.

Electronic effects II: vibrations

Vibrations of atoms and molecules in an STM junction open up additional channels for electron transport, they therefore lead to steps in the dI/dV spectrum. The change of conductance due to such a vibration typically depends on the excitation energy, which, for example, is around 200–300 meV for exciting molecular bonds in hydrocarbons. The change of the conductance is comparatively small in this case. In the 1990s it was assumed that even at Helium temperatures the measured spectrum would be too noisy to accurately measure vibrational excitations. It was the group of Wilson Ho, which first demonstrated that the obstacles to such a measurement could in fact be overcome.

In 1998, the vibrational excitation of acetylene absorbed on a copper(100) surface was measured.[130] This mechanism has since been explored extensively in systems ranging from molecular hydrogen[131] or carbon monoxide[132,133] to larger molecules like porphyrins, either in connection to the vibration of a specific bond[134] or to vibrations extended over the entire molecule,[129] and C_{60} molecules.[135] The tunnelling electrons excite low-energy mechanical vibrations which can produce similar strong spectroscopic features to magnetic excitations.[115,136–138] In addition, vibrational excitation can interact with the spin excitations,[139–141] leading to the split of the Kondo resonance in vibrational side-bands. As a result, distinguishing between the two features can be difficult.

In the previous section we identified potential misinterpretations of Kondo resonances at Helium temperatures due to the limited temperature range in the experiments. It has indeed been claimed in quite a few articles in the last ten years that Kondo resonances have been measured, even though the
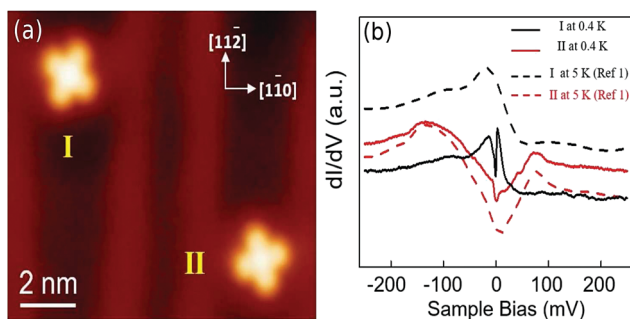

Fig. 6 (a) STM image (I = 10 pA, V_b = −0.2 V) of isolated FePc molecules in the fcc region of Au(111), showing two types of adsorption configurations. (b) dI/dV spectra (setpoint: I = 0.2 nA, V_b = −0.1 V) taken on the Fe ions for both configurations at 0.4 K and 5 K, showing dramatically different characteristic features near E_F: a dip superimposed on a broad feature for FePc (I) and broad dip with fine features for FePc (II). Adapted from Gao *et al.*[114] and Yang *et al.* (unpublished). Reproduced with permission from American Physical Society, copyright 2007.
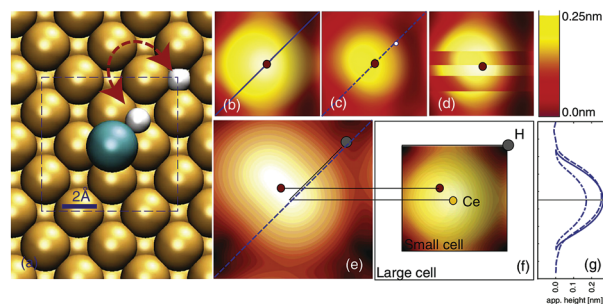

Fig. 7 (a) Diffusion of hydrogen from an Ag lattice site to Ce (see arrow). (b) Constant density contour for Ce adatom and (c) for Ce adatom with coadsorbed hydrogen. (d) The contour changes its vertical distance by more than 100 pm due to diffusion of hydrogen onto Ce. (e) Constant density contour for Ce and H at separate hollow sites of the Ag lattice. (f) Lateral shift of the contour maximum by 0.1 nm due to hydrogen at a neighbouring lattice site. The small cell refers to the calculation of Ce/Ag(100), (hydrogen: large circle, new contour maximum: small circle). Linescans (g) of the Ce and CeH feature. The linescans refer to the diagonal indicated in frames (b), (c) and (e). Adapted from Hofer *et al.*[115] with permission from IOP Publishing, copyright 2008.
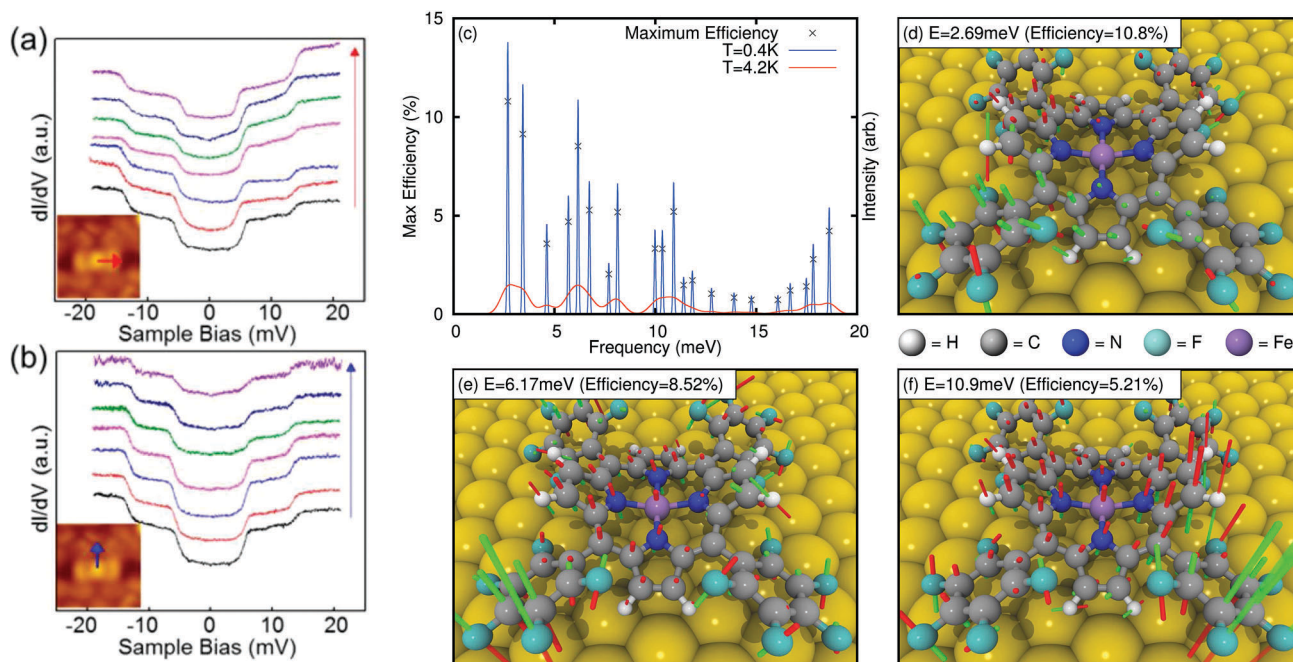
Fig. 8 Spatial distribution of IETS at 0.4 K. (a) Sequence of dI/dV signals recorded along red arrow (inset) at 0.4 K and zero magnetic field and (b) sequence of dI/dV signals recorded along blue arrow (inset) at 0.4 K and zero magnetic field ($U = -20$ mV, $I = 0.3$ nA; $V_{rms} = 0.5$ mV). The spectra from bottom to top are measured from the centre toward the edge and are vertically displaced for clarity. (c) Simulated IES, showing a number of low-lying vibrational modes in the range below 20 meV. The quantum efficiencies are then defined as the ratio of the total change in conductance and the unperturbed elastic conductance. (d–f) The oscillations for the most efficient phonon modes in the region for the first and second peak of the experimental IETS. The movement of each ion is represented by vectors (green/red) given the direction of the oscillation (positive/negative). Adapted from Chen et al.[129] with permission from American Chemical Society, copyright 2017.

Kondo temperature estimated from the shape of the Fano resonance was on the order of 100 K.[142–147] In this respect it has to be understood that vibrations at very low energy will have both, a fairly large change of conductance, and a shape which, at 4 K, looks like a dip at the Fermi level. This has first been observed in experiments with cerium atoms on a silver(111) surface.

Here, it was initially assumed that single Cerium atoms would lead to a Kondo resonance observable at 4 K.[124] This interpretation remained unchallenged until a new set of experiments and simulations found that the Kondo temperature for Cerium on silver surfaces would be too low to be observed at 4 K (it was below 1 K in the simulations[115]), and that the only possible explanation for the feature was in fact a low lying vibrational mode of a CeH molecule adsorbed on silver (see Fig. 7) This interpretation and a different explanation of the original experimental results were later confirmed in experiments at 0.5 K.[115,137]

However, we think that this might be in fact a general problem in the interpretation of data from tunneling spectroscopy experiments on two dimensional interfaces. One characteristic that is often used to distinguish between the two effects is the relative change in conductance at the IETS steps.[148–154] Typically, the largest conductance changes caused by vibration excitation reach 20%, in the cases of Ce–H[115, 131] and CO-molecular cascades,[133] because of partial cancellation of the changes of the elastic and inelastic conductances.[155] However, it has been observed that larger changes in the conductance are possible. Indeed, vibrational excitations in large molecules have recently been measured.[129] Fig. 8 shows these measurements. In (a) and (b), the step-like features in the dI/dV spectra are show to have a spatial extension over the molecule. This, along with the fact that the steps remain at the same energy under a magnetic field, is used to argue that these features are due to vibrational excitations. Fig. 8(d–f) show a schematic representation of calculated low-energy vibrations, which are extended over the entire molecule. High quantum efficiencies were calculated (c), supporting the interpretation that the spectra originate for vibrational modes. The salient feature of these extended vibrational modes is that they require smaller deformations of intramolecular bond lengths as compared to more localized oscillations, leading to much lower energies. Another distinguishing characteristic is the behaviour under a magnetic field, where it is expected that a Kondo feature will broaden due to Zeeman splitting[156–158] and a vibrational excitation will remain largely unchanged. This too has been used to help distinguish between the two features.[129,159]

Conclusion

It is often claimed that progress in science it mainly due to new experimental and theoretical methods becoming available. However, one could also say that new methods allow for new

levels of imagination to come to bear on science and technology. Today, we can create atomic and molecular interfaces close to atomically defined in our best experiments. We can also analyse the physical properties of these interfaces with methods which allow us to understand their physical characteristics with a resolution approaching 0.1 meV in the energy space, and sometimes better than 1 pm in real space. The last frontier today is probably the time domain. Here, our methods are still somewhat limited. For example, we cannot actually resolve atomic and molecular vibrations, or the pathway of an electron through a system in real time. We are limited to estimating the corresponding effects in real space and energy space. So from a very general perspective, the job, assigned to us by Richard Feynman in the 1960s, has actually been accomplished. The job left to do is to develop a detailed understanding of the intricate dynamics of molecular interfaces and harness this understanding to engineer biochemical systems from the bottom up. This is probably a task which will take us another thirty years.

Conflicts of interest

There are no conflicts to declare.

Acknowledgements

References

1 M. F. Crommie, C. P. Lutz and D. M. Eigler, *Science*, 1993, **262**, 218.
2 S.-W. Hla, K.-F. Braun and K.-H. Rieder, *Phys. Rev. B: Condens. Matter Mater. Phys.*, 2003, **67**, 201402.
3 S.-W. Hla and K.-H. Rieder, *Annu. Rev. Phys. Chem.*, 2003, **54**, 307.
4 J. V. Barth, *Annu. Rev. Phys. Chem.*, 2007, **58**, 375.
5 V. Fock, *Z. Phys.*, 1930, **61**, 126.
6 W. Hartree, *Proc. R. Soc. London, Ser. A*, 1935, **150**, 9.
7 P. Hohenberg and W. Kohn, *Phys. Rev. B: Condens. Matter Mater. Phys.*, 1964, **136**, 864.
8 W. Kohn and L. J. Sham, *Phys. Rev. A: At., Mol., Opt. Phys.*, 1965, **140**, 1133.
9 W. Kohn, *Phys. Rev. Lett.*, 1996, **76**, 3168.
10 K. Burke, *J. Chem. Phys.*, 2012, **136**, 150901.
11 R. O. Jones, *Rev. Mod. Phys.*, 2015, **87**, 897.
12 H. Hellmann, *J. Chem. Phys.*, 1935, **3**, 61.
13 W. E. Pickett, *Comput. Phys. Rep.*, 1989, **9**, 115.
14 P. Schwerdtfeger, *ChemPhysChem*, 2011, **12**, 3143.
15 D. R. Hamann, M. Schlüter and C. Chiang, *Phys. Rev. Lett.*, 1979, **43**, 1494.
16 D. Vanderbilt, *Phys. Rev. B: Condens. Matter Mater. Phys.*, 1990, **41**, 7892.
17 G. Kresse and J. Fürthmuller, *Phys. Rev. B: Condens. Matter. Phys.*, 1996, **54**, 11169.
18 D. Hobbs, G. Kresse and J. Hafner, *Phys. Rev. B: Condens. Matter Mater. Phys.*, 2000, **62**, 11556.
19 P. E. Blöchl, *Phys. Rev. B: Condens. Matter Mater. Phys.*, 1994, **50**, 17953.
20 G. Kresse and D. Joubert, *Phys. Rev. B: Condens. Matter Mater. Phys.*, 1999, **59**, 1758.
21 M. Levy, *Proc. Natl. Acad. Sci. U. S. A.*, 1979, **76**, 6062.
22 M. Levy, J. P. Perdew and V. Sahni, *Phys. Rev. A: At., Mol., Opt. Phys.*, 1984, **30**, 2745.
23 M. Pearson, E. Smargiassi and P. Madden, *J. Phys.: Condens. Matter*, 1993, **5**, 3221.
24 J. M. Soler, E. Artacho, J. D. Gale, A. García, J. Junquera, P. Ordejón and D. Sánchez-Portal, *J. Phys.: Condens. Matter*, 2002, **14**, 2745.
25 P. D. Haynes, C.-K. Skylaris, A. A. Mostofi and M. C. Payne, *Phys. Status Solidi B*, 2006, **243**, 2489.
26 W. Xiao, K-H. Ernst, K. Palotas, Y. Zhang, E. Bruyer, L. Peng, T. Greber, W. A. Hofer, L. T. Scott and R. Fasel, *Nat. Chem.*, 2016, **8**, 326.
27 V. Hallmark, S. Chiang, J. Rabolt, J. Swalen and R. Wilson, *Phys. Rev. Lett.*, 1987, **59**, 2879.
28 G. Bond, *Gold Bull.*, 1972, **5**, 11.
29 J. Barth, H. Brune, G. Ertl and R. Behm, *Phys. Rev. B: Condens. Matter Mater. Phys.*, 1990, **42**, 9307.
30 M. Haruta, *Catal. Today*, 1997, **36**, 153.
31 F. Hanke and J. Björk, *Phys. Rev. B: Condens. Matter Mater. Phys.*, 2013, **87**, 235422.
32 H. Kroto, J. Heath, S. O'brien, R. Curl and R. Smalley, *Nature*, 1985, **318**, 162.
33 E. I. Altman and R. J. Colton, *Surf. Sci.*, 1992, **279**, 49.
34 D. Fujita, T. Yakabe, H. Nejoh, T. Sato and M. Iwatsuki, *Surf. Sci.*, 1996, **366**, 93.
35 W. Xiao, P. Ruffieux, K. At-Mansour, O. Gröning, K. Palotas, W. A. Hofer, P. Gröning and R. Fasel, *J. Phys. Chem. B*, 2006, **110**, 21394.
36 N. Hauptmann, F. Mohn, L. Gross, G. Meyer, T. Frederiksen and R. Berndt, *New J. Phys.*, 2012, **14**, 073032.
37 Y. Chai, T. Guo, C. Jin, R. E. Haufler, L. F. Chibante, J. Fure, L. Wang, J. M. Alford and R. E. Smalley, *J. Phys. Chem.*, 1991, **95**, 7564.
38 P. Gambardella, *J. Phys.: Condens. Matter*, 2003, **15**, S2533.
39 C. Tegenkamp, *J. Phys.: Condens. Matter*, 2008, **21**, 013002.
40 P. Gambardella, A. Dallmeyer, K. Maiti, M. Malagoli, W. Eberhardt, K. Kern and C. Carbone, *Nature*, 2002, **416**, 301.
41 H. Fujisawa, S. Shiraki, M. Furukawa, S. Ito, T. Nakamura, T. Muro, M. Nantoh and M. Kawai, *Phys. Rev. B: Condens. Matter Mater. Phys.*, 2007, **75**, 245423.
42 H. Ding, V. Stepanyuk, P. Ignatiev, N. Negulyaev, L. Niebergall, M. Wasniowska, C. Gao, P. Bruno and J. Kirschner, *Phys. Rev. B: Condens. Matter Mater. Phys.*, 2007, **76**, 033409.
43 M. Vladimirova, M. Stengel, A. De Vita, A. Baldereschi, M. Böhringer, K. Morgenstern, R. Berndt and W.-D. Schneider, *Europhys. Lett.*, 2001, **56**, 254.
44 P. Ruffieux, K. Palotás, O. Gröning, D. Wasserfallen, K. Müllen, W. A. Hofer, P. Gröning and R. Fasel, *J. Am. Chem. Soc.*, 2007, **129**, 5007.
45 P. Samorí, N. Severin, C. D. Simpson, K. Müllen and J. P. Rabe, *J. Am. Chem. Soc.*, 2002, **124**, 9454.
46 F. Jäckel, M. D. Watson, K. Müllen and J. Rabe, *Phys. Rev. Lett.*, 2004, **92**, 188303.
47 Z. Wang, F. Dötz, V. Enkelmann and K. Müllen, *Angew. Chem.*, 2005, **117**, 1273.
48 L. Gross, F. Moresco, P. Ruffieux, A. Gourdon, C. Joachim and K.-H. Rieder, *Phys. Rev. B: Condens. Matter Mater. Phys.*, 2005, **71**, 165428.
49 P. Ruffieux, O. Gröning, R. Fasel, M. Kastler, D. Wasserfallen, K. Müllen and P. Gröning, *J. Phys. Chem. B*, 2006, **110**, 11253.
50 M. Abadía, R. González-Moreno, A. Sarasola, G. Otero-Irurueta, A. Verdini, L. Floreano, A. Garcia-Lekue and C. Rogero, *J. Phys. Chem. C*, 2014, **118**, 29704.
51 B. Göhler, V. Hamelbeck, T. Markus, M. Kettner, G. Hanne, Z. Vager, R. Naaman and H. Zacharias, *Science*, 2011, **331**, 894.
52 A.-M. Guo and Q.-f. Sun, *Phys. Rev. Lett.*, 2012, **108**, 218102.
53 R. Gutierrez, E. Díaz, R. Naaman and G. Cuniberti, *Phys. Rev. B: Condens. Matter Mater. Phys.*, 2012, **85**, 081404.
54 L. Gao, Q. Liu, Y. Zhang, N. Jiang, H. Zhang, Z. Cheng, W. Qiu, S. Du, Y. Liu and W. Hofer, *et al.*, *Phys. Rev. Lett.*, 2008, **101**, 197209.
55 L. Zhang, S. Du, J. Sun, L. Huang, L. Meng, W. Xu, L. Pan, Y. Pan, Y. Wang and W. Hofer, *et al.*, *Adv. Mater. Interfaces*, 2014, **1**, 1300104.
56 D. M. Eigler, C. Lutz and W. Rudge, *Nature*, 1991, **352**, 600.
57 H. Park, J. Park, A. K. Lim, E. H. Anderson, A. P. Alivisatos and P. L. McEuen, *Nature*, 2000, **407**, 57.
58 G. S. Kottas, L. I. Clarke, D. Horinek and J. Michl, *Chem. Rev.*, 2005, **105**, 1281.
59 B. Stipe, M. Rezaei and W. Ho, *Science*, 1998, **279**, 1907.
60 J. K. Gimzewski, C. Joachim, R. R. Schlittler, V. Langlais, H. Tang and I. Johannsen, *Science*, 1998, **281**, 531.
61 F. Chiaravalloti, L. Gross, K-H. Rieder, S. M. Stojkovic, A. Gourdon, C. Joachim and F. Moresco, *Nat. Mater.*, 2007, **6**, 30.
62 L. Grill, K-H. Rieder, F. Moresco, G. Rapenne, S. Stojkovic, X. Bouju and C. Joachim, *Nat. Nanotechnol.*, 2007, **2**, 95.
63 Z.-B. Xie, Y.-L. Wang, M.-L. Tao, K. Sun, Y.-B. Tu, H.-K. Yuan and J.-Z. Wang, *Appl. Surf. Sci.*, 2018, **439**, 462.

64 N. Wintjes, D. Bonifazi, F. Cheng, A. Kiebele, M. Stöhr, T. Jung, H. Spillmann and F. Diederich, *Angew. Chem.*, 2007, **119**, 4167.
65 D. Kühne, F. Klappenberger, W. Krenner, S. Klyatskaya, M. Ruben and J. V. Barth, *Proc. Natl. Acad. Sci. U. S. A.*, 2010, **107**, 21332.
66 C.-A. Palma, J. Björk, F. Rao, D. Kühne, F. Klappenberger and J. V. Barth, *Nano Lett.*, 2014, **14**, 4461.
67 J. A. Theobald, N. S. Oxtoby, M. A. Phillips, N. R. Champness and P. H. Beton, *Nature*, 2003, **424**, 1029.
68 S. Stepanow, M. Lingenfelder, A. Dmitriev, H. Spillmann, E. Delvigne, N. Lin, X. Deng, C. Cai, J. V. Barth and K. Kern, *Nat. Mater.*, 2004, **3**, 229.
69 H. L. Zhang, W. Chen, H. Huang, L. Chen and A. T. S. Wee, *J. Am. Chem. Soc.*, 2008, **130**, 2720.
70 Z. Cheng, J. Wyrick, M. Luo, D. Sun, D. Kim, Y. Zhu, W. Lu, K. Kim, T. Einstein and L. Bartels, *Phys. Rev. Lett.*, 2010, **105**, 066104.
71 J. Teyssandier, S. De Feyter and K. S. Mali, *Chem. Commun.*, 2016, **52**, 11465.
72 Q. Li, C. Zheng, R. Wang, B. Miao, R. Cao, L. Sun, D. Wu, Y. Wu, S. Li and B. Wang, *et al.*, *Phys. Rev. B*, 2018, **97**, 035417.
73 S. Marchini, S. Günther and J. Wintterlin, *Phys. Rev. B: Condens. Matter Mater. Phys.*, 2007, **76**, 075429.
74 B. Wang, M.-L. Bocquet, S. Marchini, S. Günther and J. Wintterlin, *Phys. Chem. Chem. Phys.*, 2008, **10**, 3530.
75 Y. Pan, H. Zhang, D. Shi, J. Sun, S. Du, F. Liu and H.-J. Gao, *Adv. Mater.*, 2009, **21**, 2777.
76 Y. Pan, M. Gao, L. Huang, F. Liu and H.-J. Gao, *Appl. Phys. Lett.*, 2009, **95**, 093106.
77 B. Wang, S. Günther, J. Wintterlin and M. Bocquet, *New J. Phys.*, 2010, **12**, 043041.
78 T. Gerber, C. Busse, J. Mysliveček, J. Coraux and T. Michely, *et al.*, *New J. Phys.*, 2009, **11**, 103045.
79 H. Zhang, Q. Fu, Y. Cui, D. Tan and X. Bao, *Chin. Sci. Bull.*, 2009, **54**, 2446.
80 K. Donner and P. Jakob, *J. Chem. Phys.*, 2009, **131**, 164701.
81 Z. Zhou, F. Gao and D. W. Goodman, *Surf. Sci.*, 2010, **604**, L31.
82 M. Sicot, S. Bouvron, O. Zander, U. Rüdiger, Y. S. Dedkov and M. Fonin, *Appl. Phys. Lett.*, 2010, **96**, 093115.
83 E. Sutter, P. Albrecht, B. Wang, M.-L. Bocquet, L. Wu, Y. Zhu and P. Sutter, *Surf. Sci.*, 2011, **605**, 1676.
84 Y. Han and J. W. Evans, *J. Chem. Phys.*, 2015, **143**, 164706.
85 A. Goriachko, Y. He, M. Knapp, H. Over, M. Corso, T. Brugger, S. Berner, J. Osterwalder and T. Greber, *Langmuir*, 2007, **23**, 2928.
86 S. Joshi, D. Ecija, R. Koitz, M. Iannuzzi, A. P. Seitsonen, J. Hutter, H. Sachdev, S. Vijayaraghavan, F. Bischoff and K. Seufert, *et al.*, *Nano Lett.*, 2012, **12**, 5821.
87 F. Schulz, R. Drost, S. K. Hämäläinen and P. Liljeroth, *ACS Nano*, 2013, **7**, 11121.
88 M. Corso, W. Auwärter, M. Muntwiler, A. Tamai, T. Greber and J. Osterwalder, *Science*, 2004, **303**, 217.
89 J. Mao, H. Zhang, Y. Jiang, Y. Pan, M. Gao, W. Xiao and H.-J. Gao, *J. Am. Chem. Soc.*, 2009, **131**, 14136.
90 H. Zhang, J. Sun, T. Low, L. Zhang, Y. Pan, Q. Liu, J. Mao, H. Zhou, H. Guo and S. Du, *et al.*, *Phys. Rev. B: Condens. Matter Mater. Phys.*, 2011, **84**, 245436.
91 D. Shi, W. Ji, B. Yang, H. Cun, S. Du, L. Chi, H. Fuchs, W. A. Hofer and H.-J. Gao, *J. Phys. Chem. C*, 2009, **113**, 17643.
92 J. Repp, F. Moresco, G. Meyer, K.-H. Rieder, P. Hyldgaard and M. Persson, *Phys. Rev. Lett.*, 2000, **85**, 2981.
93 N. Knorr, H. Brune, M. Epple, A. Hirstein, M. Schneider and K. Kern, *Phys. Rev. B: Condens. Matter Mater. Phys.*, 2002, **65**, 115420.
94 F. Silly, M. Pivetta, M. Ternes, F. Patthey, J. P. Pelz and W.-D. Schneider, *Phys. Rev. Lett.*, 2004, **92**, 016101.
95 M. Kulawik, H.-P. Rust, M. Heyde, N. Nilius, B. A. Mantooth, P. S. Weiss and H.-J. Freund, *Surf. Sci.*, 2005, **590**, L253.
96 Y. Wang, X. Ge, C. Manzano, J. Kröger, R. Berndt, W. A. Hofer, H. Tang and J. Cerda, *J. Am. Chem. Soc.*, 2009, **131**, 10400.
97 J. Friedel, *Nuovo Cimento*, 1958, **7**, 287.
98 S. U. Nanayakkara, E. C. H. Sykes, L. C. Fernández-Torres, M. M. Blake and P. S. Weiss, *Phys. Rev. Lett.*, 2007, **98**, 206108.
99 M. Pivetta, G. E. Pacchioni, E. Fernandes and H. Brune, *J. Chem. Phys.*, 2015, **142**, 101928.
100 J. Meyer, A. Nickel, R. Ohmann, C. Toher, D. A. Ryndyk, Y. Garmshausen, S. Hecht, F. Moresco and G. Cuniberti, *et al.*, *Chem. Commun.*, 2015, **51**, 12621.
101 D. Shi, W. Ji, X. Lin, X. He, J. Lian, L. Gao, J. Cai, H. Lin, S. Du and F. Lin, *et al.*, *Phys. Rev. Lett.*, 2006, **96**, 226101.

102 L. Zotti, G. Teobaldi, W. Hofer, W. Auwärter, A. Weber-Bargioni and J. Barth, *Surf. Sci.*, 2007, **601**, 2409.
103 W. Auwärter, A. Weber-Bargioni, A. Riemann, A. Schiffrin, O. Gröning, R. Fasel and J. Barth, *J. Chem. Phys.*, 2006, **124**, 194708.
104 H. Cun, Y. Wang, S. Du, L. Zhang, L. Zhang, B. Yang, X. He, Y. Wang, X. Zhu and Q. Yuan, *et al.*, *Nano Lett.*, 2012, **12**, 1229.
105 M. E. Kassner, S. Nemat-Nasser, Z. Suo, G. Bao, J. C. Barbour, L. C. Brinson, H. Espinosa, H. Gao, S. Granick, P. Gumbsch, K.-S. Kim, W. Knauss, L. Kubin, J. Langer, B. C. Larson, L. Mahadevan, A. Majumdar, S. Torquato and F. Van Swol, *Mech. Mater.*, 2005, **37**, 231.
106 X. Zhang, C. Neumann, P. Angelova, A. Beyer and A. Gölzhäuser, *Langmuir*, 2014, **30**, 8221.
107 D. Sun, D.-H. Kim, D. Le, Ø. Borck, K. Berland, K. Kim, W. Lu, Y. Zhu, M. Luo and J. Wyrick, *et al.*, *Phys. Rev. B: Condens. Matter Mater. Phys.*, 2010, **82**, 201410.
108 Y. Wang, J. Kröger, R. Berndt and W. Hofer, *Angew. Chem.*, 2009, **48**, 1261.
109 M. Lackinger and M. Hietschold, *Surf. Sci.*, 2002, **520**, L619.
110 C. Stadler, S. Hansen, F. Pollinger, C. Kumpf, E. Umbach, T.-L. Lee and J. Zegenhagen, *Phys. Rev. B: Condens. Matter Mater. Phys.*, 2006, **74**, 035404.
111 C. Stadler, S. Hansen, I. Kröger, C. Kumpf and E. Umbach, *Nat. Phys.*, 2009, **5**, 153.
112 M. Toader and M. Hietschold, *J. Phys. Chem. C*, 2011, **115**, 3099.
113 Y. Wang, J. Kröger, R. Berndt and H. Tang, *J. Am. Chem. Soc.*, 2010, **132**, 12546.
114 L. Gao, W. Ji, Y. Hu, Z. Cheng, Z. Deng, Q. Liu, N. Jiang, X. Lin, W. Guo, S. Du, W. A. Hofer, X. Xie and H. Gao, *et al.*, *Phys. Rev. Lett.*, 2007, **99**, 106402.
115 W. A. Hofer, G. Teobaldi and N. Lorente, *Nanotechnology*, 2008, **19**, 305701.
116 W. Xiao, D. Passerone, P. Ruffieux, K. Aït-Mansour, O. Gröning, E. Tosatti, J. S. Siegel and R. Fasel, *J. Am. Chem. Soc.*, 2008, **130**, 4767.
117 T. Samuely, S.-X. Liu, M. Haas, S. Decurtins, T. A. Jung and M. Stöhr, *J. Phys. Chem. C*, 2009, **113**, 19373.
118 S. Vijayaraghavan, D. Écija, W. Auwärter, S. Joshi, K. Seufert, A. P. Seitsonen, K. Tashiro and J. V. Barth, *Nano Lett.*, 2012, **12**, 4077.
119 C. R. Dean, A. F. Young, I. Meric, C. Lee, L. Wang, S. Sorgenfrei, K. Watanabe, T. Taniguchi, P. Kim and K. L. Shepard, *et al.*, *Nat. Nanotechnol.*, 2010, **5**, 722.
120 J. Xue, J. Sanchez-Yamagishi, D. Bulmash, P. Jacquod, A. Deshpande, K. Watanabe, T. Taniguchi, P. Jarillo-Herrero and B. J. LeRoy, *Nat. Mater.*, 2011, **10**, 282.
121 H. Terrones, F. López-Urías and M. Terrones, *Sci. Rep.*, 2013, **3**, 1549.
122 V. Madhavan, W. Chen, T. Jamneala, M. Crommie and N. Wingreen, *Science*, 1998, **280**, 567.
123 U. Fano, *Phys. Rev.*, 1961, **124**, 1866.
124 J. Li, W.-D. Schneider, R. Berndt and B. Delley, *Phys. Rev. Lett.*, 1998, **80**, 2893.
125 T. Jamneala, V. Madhavan, W. Chen and M. Crommie, *Phys. Rev. B: Condens. Matter Mater. Phys.*, 2000, **61**, 9990.
126 V. Madhavan, W. Chen, T. Jamneala, M. Crommie and N. S. Wingreen, *Phys. Rev. B: Condens. Matter Mater. Phys.*, 2001, **64**, 165412.
127 Y. J. Song, A. F. Otte, V. Shvarts, Z. Zhao, Y. Kuk, S. R. Blankenship, A. Band, F. M. Hess and J. A. Stroscio, *Rev. Sci. Instrum.*, 2010, **81**, 121101.
128 N. Tsukahara, S. Shiraki, S. Itou, N. Ohta, N. Takagi and M. Kawai, *Phys. Rev. Lett.*, 2011, **106**, 187201.
129 H. Chen, T. Pope, Z.-Y. Wu, D. Wang, L. Tao, D.-L. Bao, W. Xiao, J.-L. Zhang, Y.-Y. Zhang and S. Du, *et al.*, *Nano Lett.*, 2017, **17**, 4929.
130 B. Stipe, M. Rezaei and W. Ho, *Science*, 1998, **280**, 1732.
131 M. Pivetta, M. Ternes, F. Patthey and W.-D. Schneider, *Phys. Rev. Lett.*, 2007, **99**, 126104.
132 L. Lauhon and W. Ho, *Phys. Rev. B: Condens. Matter Mater. Phys.*, 1999, **60**, R8525.
133 A. Heinrich, C. Lutz, J. Gupta and D. Eigler, *Science*, 2002, **298**, 1381.
134 T. Wallis, X. Chen and W. Ho, *J. Chem. Phys.*, 2000, **113**, 4837.
135 K. J. Franke and J. I. Pascual, *J. Phys.: Condens. Matter*, 2012, **24**, 394002.
136 J. Gupta, C. Lutz, A. Heinrich and D. Eigler, *Phys. Rev. B: Condens. Matter Mater. Phys.*, 2005, **71**, 115416.
137 M. Ternes, A. J. Heinrich and W.-D. Schneider, *J. Phys.: Condens. Matter*, 2008, **21**, 053001.

138 F. D. Natterer, F. Patthey and H. Brune, *Phys. Rev. Lett.*, 2013, **111**, 175303.

139 I. Fernández-Torrente, K. Franke and J. Pascual, *Phys. Rev. Lett.*, 2008, **101**, 217203.

140 F. May, M. R. Wegewijs and W. Hofstetter, *Beilstein J. Nanotechnol.*, 2011, **2**, 693.

141 A. Kenawy, J. Splettstoesser and M. Misiorny, *AIP Adv.*, 2017, **7**, 055708.

142 Y.-S. Fu, S.-H. Ji, X. Chen, X.-C. Ma, R. Wu, C.-C. Wang, W.-H. Duan, X.-H. Qiu, B. Sun and P. Zhang, *et al.*, *Phys. Rev. Lett.*, 2007, **99**, 256601.

143 U. Perera, H. Kulik, V. Iancu, L. D. Da Silva, S. Ulloa, N. Marzari and S.-W. Hla, *Phys. Rev. Lett.*, 2010, **105**, 106601.

144 J. Kügel, M. Karolak, J. Senkpiel, P.-J. Hsu, G. Sangiovanni and M. Bode, *Nano Lett.*, 2014, **14**, 3895.

145 J. Kügel, M. Karolak, A. Krönlein, J. Senkpiel, P.-J. Hsu, G. Sangiovanni and M. Bode, *Phys. Rev. B: Condens. Matter Mater. Phys.*, 2015, **91**, 235130.

146 Y. Wang, X. Zheng and J. Yang, *Phys. Rev. B*, 2016, **93**, 125114.

147 G. E. Pacchioni, M. Pivetta, L. Gragnaniello, F. Donati, G. Autès, O. V. Yazyev, S. Rusponi and H. Brune, *ACS Nano*, 2017, **11**, 2675.

148 X. Chen, Y.-S. Fu, S.-H. Ji, T. Zhang, P. Cheng, X.-C. Ma, X.-L. Zou, W.-H. Duan, J.-F. Jia and Q.-K. Xue, *Phys. Rev. Lett.*, 2008, **101**, 197208.

149 N. Tsukahara, K.-I. Noto, M. Ohara, S. Shiraki, N. Takagi, Y. Takata, J. Miyawaki, M. Taguchi, A. Chainani and S. Shin, *et al.*, *Phys. Rev. Lett.*, 2009, **102**, 167203.

150 J.-P. Gauyacq, F. D. Novaes and N. Lorente, *Phys. Rev. B: Condens. Matter Mater. Phys.*, 2010, **81**, 165423.

151 J.-P. Gauyacq, N. Lorente and F. D. Novaes, *Prog. Surf. Sci.*, 2012, **87**, 63.

152 B. W. Heinrich, G. Ahmadi, V. L. Müller, L. Braun, J. I. Pascual and K. J. Franke, *Nano Lett.*, 2013, **13**, 4840.

153 S. Meierott, N. Néel and J. Kröger, *Phys. Rev. B: Condens. Matter Mater. Phys.*, 2015, **91**, 201111.

154 S. Karan, C. García, M. Karolak, D. Jacob, N. Lorente and R. Berndt, *Nano Lett.*, 2018, **18**, 88.

155 K. Morgenstern, N. Lorente and K.-H. Rieder, *Phys. Status Solidi B*, 2013, **250**, 1671.

156 S. M. Cronenwett, T. H. Oosterkamp and L. P. Kouwenhoven, *Science*, 1998, **281**, 540.

157 D. Goldhaber-Gordon, H. Shtrikman, D. Mahalu, D. Abusch-Magder, U. Meirav and M. Kastner, *Nature*, 1998, **391**, 156.

158 A. Heinrich, J. Gupta, C. Lutz and D. Eigler, *Science*, 2004, **306**, 466.

159 S. Karan, N. Li, Y. Zhang, Y. He, I.-P. Hong, H. Song, J.-T. Lü, Y. Wang, L. Peng and K. Wu, *et al.*, *Phys. Rev. Lett.*, 2016, **116**, 027201.